Supplementary Information for:

Fabrication of Graphene Quantum Dots *via* Size-selsctive Precipitation and Their Application in Upconversion-based DSSCs

Eunwoo Lee, Jaehoon Ryu, and Jyongsik Jang*

World Class University (WCU) program of Chemical Convergence for Energy & Environment (C_2E_2), School of Chemical and Biological Engineering, College of Engineering, Seoul National University (SNU), Seoul 151-742, Korea.

[*] E-mail: jsjang@plaza.snu.ac.kr
Tel.: +82-2-880-7069
Fax: +82-2-888-1604

1. Experimental Section

***Materials*:** Carbon nanofiber (NEXCARB-H,) was purchased from Suntel Co. and used as received. Poly(ethylene oxide) (PEO; M_w: 10,000) was purchased from Aldrich Chemical Co. and used without further purification.

***Fabrication of graphene quantum dots*:** H-CNFs (0.30 g) were added into a mixture of concentrated H_2SO_4 (60 mL) and HNO_3 (20 mL). The solution was sonicated for two hours and stirred for 24 hours at different temperatures of 80, 100, and 120 °C, respectively. The mixture was cooled and diluted with deionized (DI) water (800 mL). The pH was adjusted to 8 with Na_2CO_3. In a typical reaction, 2g of PEG (MW: 10,000) was mixed with the cutting HCNF solution, and the mixture was substantially mixed. The mixture solution was heated at 120 °C for 1 h in an autoclave and then cooled to room temperature. In order to isolate the graphene quantum dots, the size-selective precipitation has been carried out from the reaction mixture. At first, the crude solution of GQDs has been concentrated to approximately one fifth of the initial volume. After that, a nonsolvent (ethanol) has been added to the concentrated solution in volume ratio of 2:1. Then, the Na_2SO_4 salts and large sized graphenes started to precipitate. From the resulting turbid solution, the precipitate and the supernatant were separated by centrifugation at 12,000 RPM for 1hr. To the first supernatant obtained from this procedure, ethanol was added into the GQD aqueous solution in volume ratio of 2:1 and a centrifugation was performed with 12,000 RPM for 1 hr, producing another fraction of supernatants and precipitates. This process was repeated several times in order to obtain fractions of GQDs with a uniform size. The obtained supernatant of GQD solution was strongly fluorescent with a uniform size. The obtained supernatant of GQD solution was strongly fluorescent with a uniform size.

Fabrication of quantum dots deposited photoanodes: Single layer film composed of 11 μm TiO_2 layer was prepared by screen-printing of P25 based TiO_2 paste on FTO-type TCO glass and sintered at 450 °C in air for 30 min. For the deposition of GQDs, the as-prepared GQD solution was spin-coated on top of the as-prepared nanoporous TiO_2 layer at 500 rpm for 20 sec from a solution with a concentration of approx. 0.5 mg/ml. The as-prepared TiO_2/GQDs films were treated with a 40 mM titanium tetrachloride ($TiCl_4$) solution and heated at 450 °C in air for 30 min before use.

Assembly of DSSCs with quantum dots deposited photoanodes: The GQDs deposited TiO_2 thin film was immersed in the dye solution (0.5 mM D719 dye in acetonitrile and t-butanol (volume ratio of 1 : 1)) for 36 h at 25 °C. For the preparation of Pt-counter electrode, a drop of 5 mM H_2PtCl_6 ethanol solution was spread out onto the FTO glasses, and thermal treated at 400 °C for 15 min under air. The working electrodes were assembled

with Pt-FTO electrodes into sandwich- type cells using thermal adhesive films (Surlyn: 60 μm, Dupont). A drop of electrolyte (Iodolyte AN-50, Solaronix), consisting of 50 mM triiodide, 0.1 M LiI, and 0.5 M 1,2-dimethyl-3-propylimidazolium iodide in acetonitrile, was injected into the cell.

***Characterization*:** For Raman analyses, a GQD solution was deposited onto a Si wafer using screen printing (Sunmechanix, SM-S550) and drop casting. FT-IR spectra of the synthesized GQD film were acquired using a Bomem MB 100 spectrometer. Photoluminescence quantum yields of GQDs in water were calculated by comparing their integrated emission to that of the water solution of rhodamine 6G. Morphological images of GQDs were acquired using transmission electron microscopy (TEM, JEOL EM-2000 EX II microscope, Japan). Incident photon-to-electron conversion efficiency (IPCE) was measured using a Solar Cell Spectral Response QE/IPCE Measurement System (QEX7, PV Measurements, Inc. Boulder, USA) from 300 nm to 1000 nm under the global AM 1.5 solar emission spectrum. The size distribution and zeta potential of GQDs were measured by using a ELS-8000 instrument (Otsuka Electronics, Japan).

2. Characterization of as-synthesized GQDs

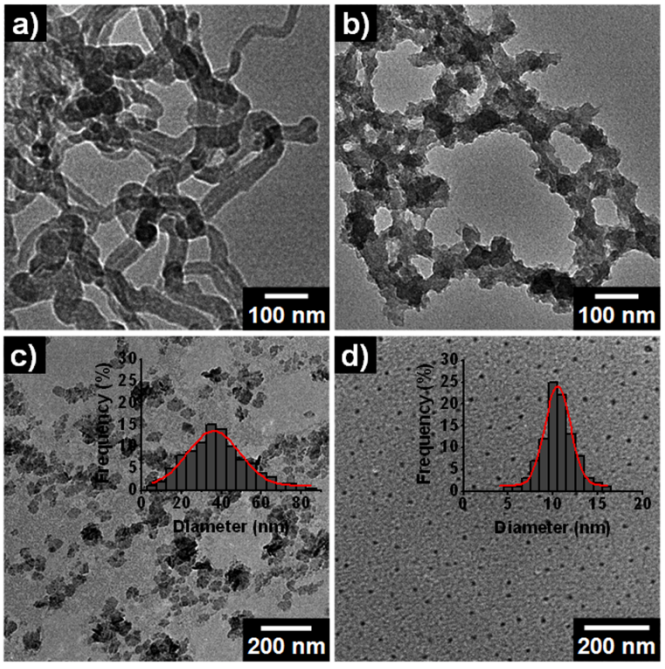

Figure S1. TEM images (a-d) for oxidized herringbone type carbon nanofibers (H-CNFs) as a function of oxidization time: (a) pristine H-CNFs, (b) h_{ox}= 6 h, (c) h_{ox}= 14 h, (d) h_{ox}= 24 h (insets: the histogram of the average GQD size which is determined by TEM (100 particles counted) and HR-TEM images.

Table S1. Physical parameters and sedimentation velocity of GQDs.

	10-nm GQD	**40-nm GQD**
Diameter [a]	*ca*. 10 nm	*ca*. 40 nm
Density [b]	1.15 g/cm^3	2.37 g/cm^3
Fluid density [c]	0.789 g/cm^3	0.789 g/cm^3
Fluid viscosity [c]	0.0012 Pa·s	0.0012 Pa·s
Sedimentation velocity [d]	1.64 x 10^{-11} m/s	1.15 x 10^{-9} m/s

[a] The average diameter of GQDs was determined by TEM (50 GQDs counted). [b] The density of GQDs was obtained using density hydrometer at a standard temperature of 20 ºC. [c] Ethanol was used as a dispersing medium. [d] Stoke's settling equation was used for calculation of sedimentation velocity. GQD Reynolds number less than 0.2.

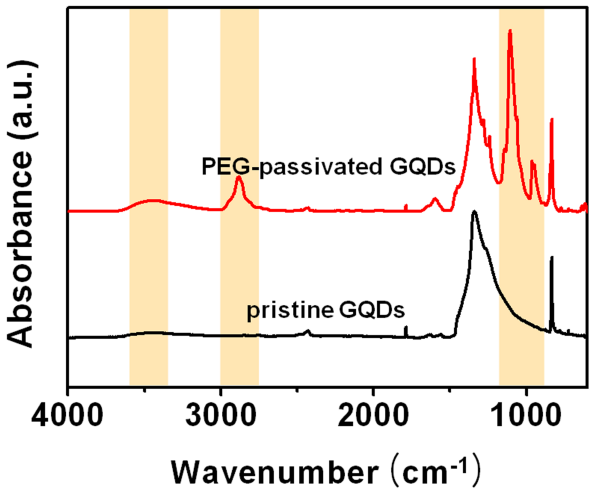

Figure S2. Fourier transform infrared (FT-IR) spectra of pristine GQDs and PEG-passivated GQDs.

Table S2. FT-IR assignments of pristine GQDs and PEG-passivated GQDs.

Samples	Wavenumber(cm^{-1})	Assignments
Pristine GQD	835	C–H deformation
	1100, 1360	C–O stretching
	1637	C=C aromatic stretching
	1785	C=O stretching
PEG-passivated GQD	835, 950	C–H deformation
	1100, 1360	C–O stretching
	1637	C=C aromatic stretching
	1785	C=O stretching
	2882	C–H stretching
	3434	O–H bending

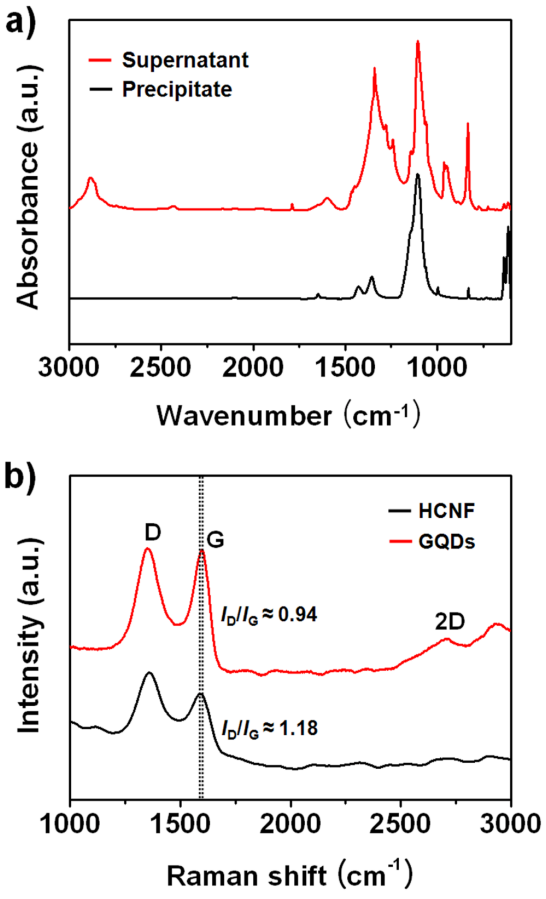

Figure S3. (a) FT-IR spectra of supernatant and precipitate after size-selective precipitation process. (b) Raman spectra of pristine HCNF and GQDs

Table S3. FT-IR assignments of precipitate and supernatant after size-selective precipitation.

Samples	Wavenumber(cm^{-1})	Assignments
Precipitate	618, 640	SO_4 asymmetric bending
	1100	SO_4 symmetric stretching
	3449	O–H stretching
Supernatant	835, 950	C–H deformation
	1100, 1360	C–O stretching
	1591	C=C aromatic stretching
	1785	C=O stretching
	2882	C–H stretching

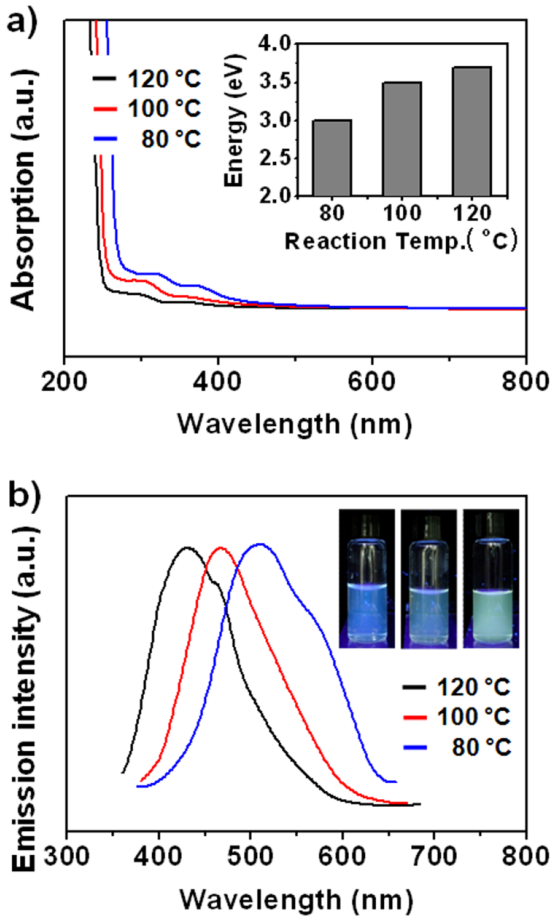

Figure S4. (a) The UV-Vis absorption spectra of the as-prepared GQDs with different oxidation temperatures (inset: the relationship between the energy gap of GQDs and the oxidation temperatures) (b) PL spectra of GQDs with different oxidation temperatures (80, 100, 120 °C), which were excited at 350 nm.

Table S4. Summary of the graphene quantum dots; synthetic temperature, average diameters, emission maxima, and emission quantum yields (QY).

Sample	Oxidation temperature (°C)	Average diameter (nm)	Emission maxima [a] (nm)	Emission quantum yield [b] (%)
GQD (80 °C)	80	10	525	23.1
GQD (100 °C)	100	8	470	25.4
GQD (120 °C)	120	6	427	26.2

[a] Emission spectra of the aforementioned upon exciting at 350 nm with emission maxima were normalized at their intensities. [b] Quantum yield measurements were obtained using Rhodamine 6G as a reference.

Table S5. Emission quantum yields (QY) of GQDs before and after the surface passivation with PEG.

Sample	Emission quantum yield [a]		Delta [c]
	Before passivation(%)	After passivation(%) [b]	(%)
GQD (80 °C)	8.3	23.1	278
GQD (100 °C)	8.8	25.4	289
GQD (120 °C)	10.2	26.2	257

[a] Quantum yield measurements were obtained using Rhodamine 6G as a reference. [b] Poly(ethylene glycol) (M.W: 10,000) was used for passivation agent. [c] An increased percentage of QY for the PEG-passivated GQDs compared with pristine GQDs.

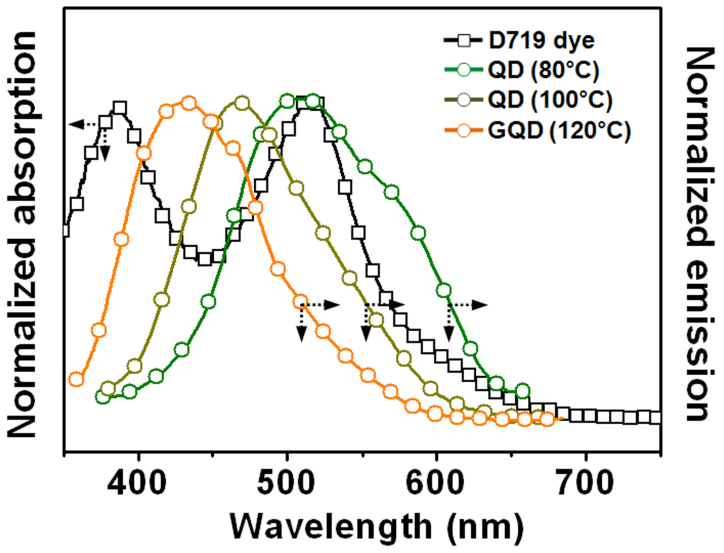

Figure S5. Absorption (left) of D719 dye and emission (right) of three types of GQDs; 80°C-, 100°C, and 120°C-oxidized GQDs. Emission spectra upon excitation at 350 nm with emission maxima normalized at their intensities.

The extent of spectral overlap of the emission spectrum of the donor with the absorption spectrum of the acceptor was analyzed by spectral overlap integral. The overlap region of 80°C-GQD+dye, 100°C-GQD+dye, and 120°C-GQD+dye are calculated to 11,307, 9,982, and 9,172, respectively. Accordingly, the degree of overlap region followed the order of 80°C-GQD+dye > 100°C-GQD+dye > 120°C-GQD+dye, which result is in accordance with the photovoltaic performance of GQD layer modified DSSC with different GQD configurations in Figure S10.

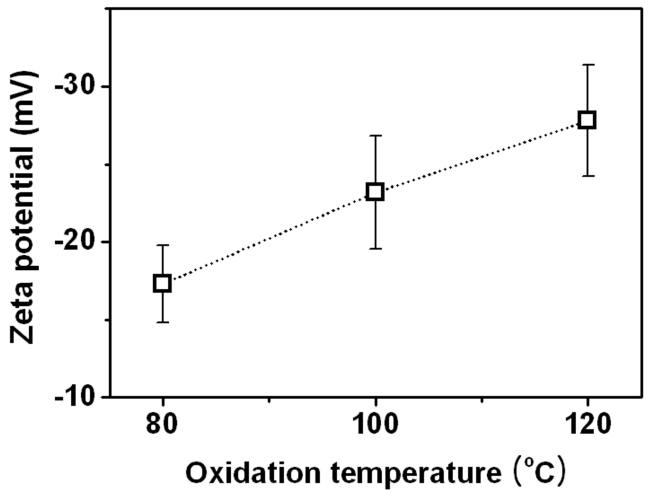

Figure S6. Plot of zeta potential *vs.* GQD samples with different oxidation levels. Smoluchowski approximation was used for the conversion equation of zeta-potential.

Under our experimental condition, the zeta potential measurements show a linear increase in the zeta potential with respect to increasing oxidation levels. The zeta potential values of 80°C-, 100°C- and 120°C-oxidized GQDs were found to be -17.3, -23.2, and -27.8 mV, respectively. The negative zeta potential values are due to the presence of electronegative functional groups formed at the graphite lattice during the oxidation process.[1] With the successive increase in the oxidation temperature, a greater number of electronegative functional groups are formed in GQD resulting in the increase of the zeta potential at higher oxidation levels. Accordingly, the results for the high oxygenated functional groups with higher zeta potential in an aqueous medium is more likely due to the dissociation of a greater number of acidic groups at the surface thereby resulting in a higher zeta potential.

[1] K. Krishnamoorthy, M. Veerapandian, K. Yun, S. J. Kim. *Carbon* **2013**, 53, 38-49.

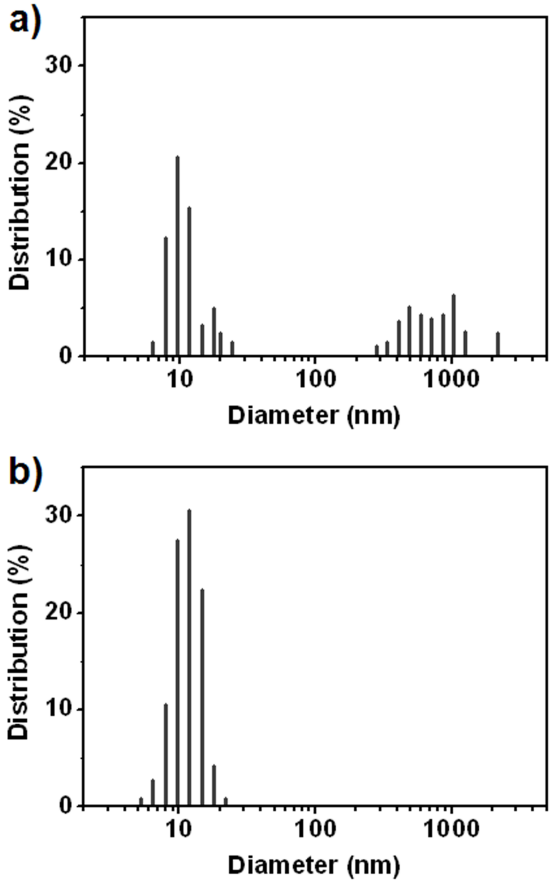

Figure S7. Size distribution of (a) GQDs (80 °C) before separation and (b) GQDs (80 °C) after separation process measured by Dynamic light scattering spectroscopy(DLS).

We investigated the size distribution of GQDs before and after the size-selective precipitation process using dynamic light scattering(DLS) analysis in **Figure S7**. Under our experimental condition, the GQDs before separation showed broad distribution in the range of 6 nm to 3 μm. However, GQDs after separation process showed narrow distribution with 12 nm peak. This result is corresponding to the results from TEM measurement in **Figure 1**.

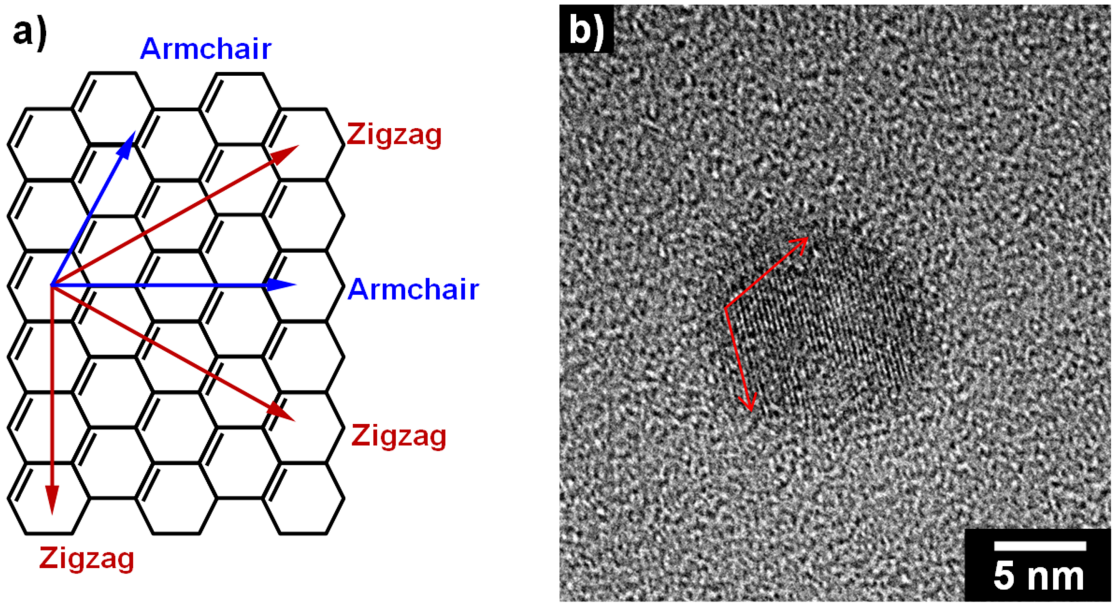

Figure S8. (a) Schematic illustration for the orientation of the hexagonal carbon network and the relative directions of zigzag and armchair. (b) HR-TEM images of the as-synthesized GQD. Red arrows indicate zigzag orientation.

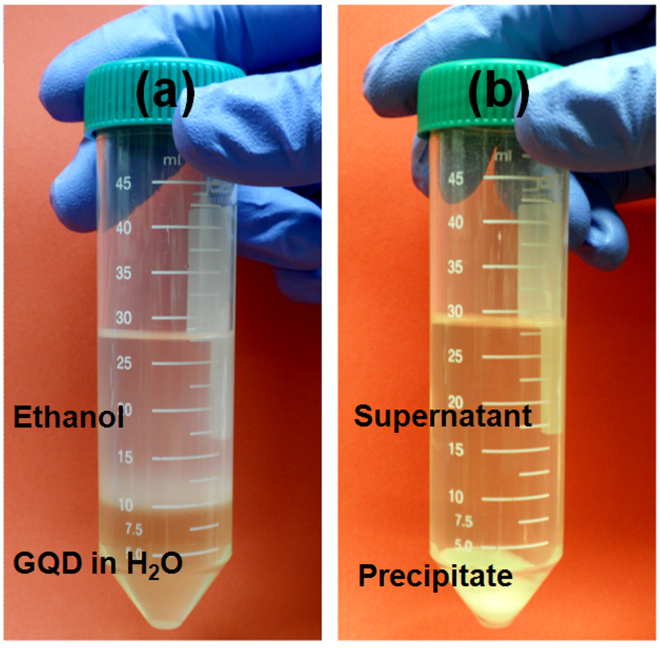

Figure S9. Photograph of GQD solutions (a) before and (b) after separation process.

3. Photovoltaic performance of GQD-layer-modified DSSCs

Table S6. Summary of photovoltaic performance of TiO_2/dye/GQD cells as a function of GQD content from 1.3 to 5.2 mg

Sample [a]	GQDs (mg)	J_{sc} [b] (mA cm^{-2})	V_{oc} [c] (mV)	FF [d]	η [e] (%)
Pristine DSSC	-	13.90	765	0.75	7.28
TiO_2/dye/GQDs cell	1.3	14.81	765	0.75	7.75
TiO_2/dye/GQDs cell	2.6	15.20	766	0.75	7.95
TiO_2/dye/GQDs cell	3.9	14.85	764	0.74	7.76
TiO_2/dye/GQDs cell	5.2	14.35	764	0.74	7.49

[a] The content of deposited GQD was varied from 0 to 5.2 mg *via* the number of spincoating . Active area of the assembled DSSC is 0.25 cm^2. [b] Short-circuit current. [c] Open-circuit voltage. [d] Fill factor. [e] Power conversion efficiency.

Table S6 demonstrates the summary of photovoltaic performance of GQD-layer modified DSSCs with the content of GQDs. Although no significant trends in open-circuit voltage (V_{oc}) and fill factor (FF) were observed, the circuit density (J_{sc}) of GQD-layer modified DSSC was significantly higher than that of the pristine DSSCs. The higher J_{sc} of GQD-layer modified DSSC than the pristine DSSC is attributable to the enhanced ability of the GQD-layer modified photoanode to harvest light by means of FRET. In addition, the J_{sc} increased as the GQD content increased to 2.6 mg, and J_{sc} decreased with greater GQD content. The decrease in J_{sc} can be explained by the formation of a PEG layer on top of the TiO_2/dye layer, which inhibited contact between the electrolyte and the dye. Therefore, a greater amount of GQDs decreased J_{sc} significantly. When 2.6 mg of GQDs were incorporated into the DSSCs, the power-conversion efficiency was enhanced to 7.95%, compared to 7.28% for pristine DSSCs.

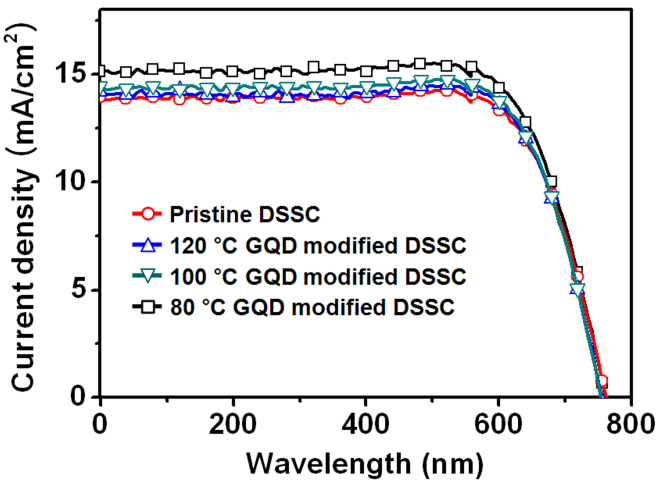

Figure S10. *J-V* curves of GQDs-modified DSSC with different types of GQDs. (80 °C, 100 °C, and 120 °C-oxidized GQDs)

Table S7. Summary of photovoltaic performance of GQD-modified DSSCs with different types of GQDs. (80 °C, 100 °C, and 120 °C-oxidized GQDs)

Sample [a]	J_{sc} [b] (mA cm^{-2})	V_{oc} [c] (mV)	*FF* [d]	η [e] (%)
Pristine DSSC	13.90	765	0.75	7.28
80°C GQD-modified DSSC	15.20	766	0.75	7.95
100°C GQD-modified DSSC	14.20	766	0.75	7.45
120°C GQD-modified DSSC	14.15	764	0.74	7.31

[a] The content of deposited GQD in GQD-modified cells was fixed to 2.6 mg. Active area of the assembled DSSC is 0.25 cm^2. [b] Short-circuit current. [c] Open-circuit voltage. [d] Fill factor. [e] Power conversion efficiency.

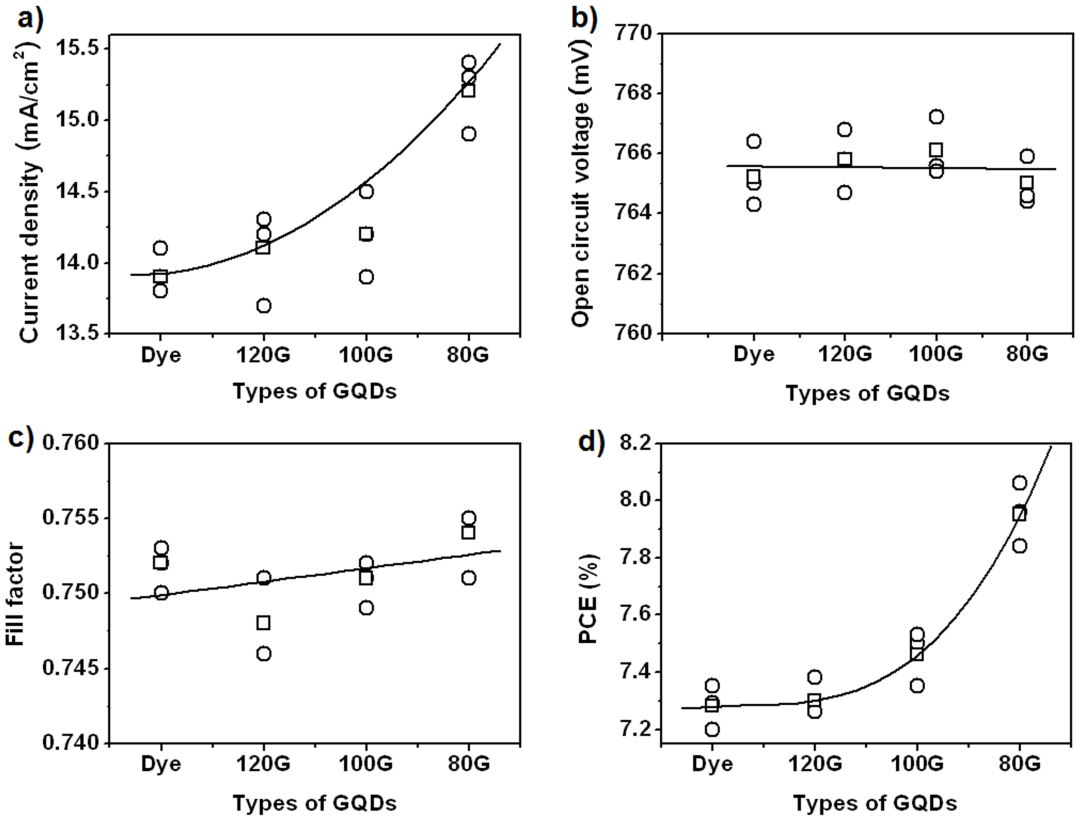

Figure S11. Photovoltaic-characteristics relationship with GQD types of GQD-layer modified DSSCs: (a) J_{sc}, (b) V_{oc}, (c) *FF* and (d) power conversion efficiency. The deposited amount of GQDs was fixed to 2.6 mg for GQD-modified layer.